TITLE: Preclinical development of CD38-targeted [89Zr]Zr-DFO-daratumumab for imaging multiple myeloma

Anchal Ghai[1], Dolonchampa Maji[1,2], Nicholas Cho[1,2], Chantiya Chanswangphuwana[3], Michael Rettig[3], John DiPersio[3], Walter Akers[4], Farrokh Dehdashti[1], Samuel Achilefu[1,2,5], Ravi Vij[3] and Monica Shokeen*[1,2]

[1]Department of Radiology, Washington University School of Medicine, St. Louis, MO

[2]Department of Biomedical Engineering, Washington University in St. Louis, St. Louis, MO

[3]Department of Medicine, Washington University School of Medicine, St. Louis, MO

[4]Center for In Vivo Imaging and Therapeutics, St. Jude Children's Research Hospital, Memphis, TN

[5]Department of Biochemistry and Molecular Biophysics, Washington University School of Medicine, St. Louis, MO

* Monica Shokeen, Department of Radiology, Mallinckrodt Institute of Radiology, 4515 McKinley Avenue, 2nd floor, St Louis, MO 63110. Phone: 1-314-362-8979; Fax: 314-747-5191 Email: mshokeen@wustl.edu

Abstract. Multiple myeloma (MM) is a plasma B-cell hematologic cancer that causes significant skeletal morbidity. Despite improvements in survival, heterogeneity in response remains a major challenge in MM. Cluster of differentiation 38 (CD38) is a type II transmembrane glycoprotein over-expressed in myeloma cells and is implicated in MM cell signaling. Daratumumab is US Food and Drug Administration approved high-affinity monoclonal antibody targeting CD38 that is clinically benefiting refractory MM patients. Here, we evaluated [89Zr]Zr-DFO-daratumumab positron emission tomography/computed tomography (PET/CT) imaging in MM tumor models.

Methods: Daratumumab was conjugated to desferrioxamine-p-benzyl-isothiocyanate (DFO-Bz-NCS) for radiolabeling with Zr-89. Chelator conjugation was confirmed by electrospray ionization-mass spectrometry (ESI-MS), and radiolabeling was monitored by instant thin-layer chromatography. Daratumumab was additionally conjugated to Cyanine5 (Cy5) dye for cell microscopy. *In vitro* and *in vivo* evaluation of [89Zr]Zr-DFO-daratumumab was performed using CD38+ human myeloma MM1.S-*luciferase* (MM1.S) cells. Cellular studies determined the affinity, immunoreactivity, and specificity of [89Zr]Zr-DFO-daratumumab. CD38^{low} 5TGM1-*luciferase* (5TGM1) murine MM cells served as negative controls. [89Zr]Zr-DFO-daratumumab PET/CT small animal imaging was performed in severe combined immunodeficient (SCID) mice bearing solid and disseminated MM tumors. Tissue biodistribution (7 days after tracer administration, 1.11 MBq/animal, n=4-6/group) was performed in wild-type and MM1.S tumor-bearing SCID mice.

Results: Specific activity of 55.5 MBq/nmol (0.37 MBq/μg) was reproducibly obtained with ^{89}Zr-daratumumab-DFO. Flow cytometry confirmed CD38 expression (>99%) on the surface of MM1.S cells. Confocal microscopy with daratumumab-Cy5 demonstrated specific cell binding. A dissociation constant, K_d: 3.3 nM (± 0.58) and receptor density, B_{max}: 10.1 fmol/mg (±0.64) was obtained with saturation binding assay. [89Zr]Zr-DFO-daratumumab/PET demonstrated specificity and sensitivity for detecting CD38+ myeloma tumors of variable sizes (8.5 to 128 mm^3) with standardized uptake values ranging from 2.1 to 9.3. Discrete medullar lesions, confirmed by

bioluminescence images, were efficiently imaged with [89Zr]Zr-DFO-daratumumab/PET. Biodistribution at seven days post administration of [89Zr]Zr-DFO-daratumumab showed prominent tumor uptake (27.7 ± 7.6 %ID/g). *In vivo* blocking was achieved with a 200-fold excess of unlabeled daratumumab.

Conclusion: [89Zr]Zr-DFO- and Cy5-daratumumab demonstrated superb binding to CD38$^+$ human MM cells and significantly low binding to CD38^{low} MM cells. Daratumumab bio-conjugates are being evaluated for image guided delivery of therapeutic radionuclides.

Keywords: [89Zr]Zr-DFO-daratumumab, cluster of differentiation 38 (CD38), multiple myeloma (MM), molecular imaging

Running Title: [89Zr]Zr-DFO-daratumumab/PET for MM

INTRODUCTION

MM is an age-related hematological malignancy of antibody-secreting plasma B-cells with over thirty thousand new cases and thirteen thousand deaths in 2016 alone *(1)*. MM remains an incurable disease demonstrating broad spectrum of aggression and resistance to treatment as a result of the genomic instability and clonal heterogeneity *(2)*. The risk of skeletal related events such as fractures is very high in MM patients and continues to rise even with treatment *(3)*. Advances in combination therapies, the advent of novel drugs such as proteasome inhibitors and immunomodulatory agents as well as the success of stem cell transplantation, has contributed to improvements in the five-year survival rate in MM *(4)*. However, the new therapies have not completely displaced the routine use of conventional chemotherapies, and the response is not uniform among MM patients. Therefore, there is an unmet need for innovative and personalized therapeutic approaches that will improve MM outcome, reduce toxicity and induce long term deep tumor regression. Recently treatment with monoclonal antibodies against antigens that are overexpressed in myeloma cells has demonstrated promising results *(5)*. Antibodies are characterized by exquisite target specificity and are therefore ideal for targeting cell-surface proteins that are selectively expressed on malignant cells *(6)*. Also, owing to too high target affinity and specificity, antibodies can exert both cytotoxic and cytostatic properties by interfering with mechanisms involved in cell growth or signaling after binding to the target. For example, antibodies can induce tumor cell death through apoptosis or multiple immune-mediated mechanisms such as complement dependent cytotoxicity, antibody-dependent cellular phagocytosis, and antibody-dependent cellular cytotoxicity.

All of these requirements are met by CD38 *(7)*. CD38 is a single chain type II transmembrane glycoprotein that has 256 amino acids in the extracellular domain, which act as an ectoenzyme, while the functional unit is a dimer with its central portion hosting the catalytic site *(8)*. CD38 is expressed on terminally differentiated plasma cells as well as on the cell surface of lymphoid

tumors such as MM, AIDS (acquired immunodeficiency syndrome)-associated lymphomas, and post-transplant lymphoproliferative disorders *(9)*. The relatively high expression of CD38 on malignant plasma cells in combination with its role in modulating intracellular signaling make it an attractive therapeutic antibody target for treatment of MM *(10)*.

Daratumumab is US Food and Drug Administration approved humanized IgG1 Kappa monoclonal antibody that targets the CD38 epitope *(11)*. Daratumumab binds to two β strands of CD38 containing amino acids 233-246 and 267-280 and is believed to demonstrate broad spectrum killing activity against CD38-expressing tumor cells by inducing tumor cell death through apoptosis and multiple immune mediated mechanisms *(12)*. Daratumumab has shown favorable safety profile and encouraging efficacy in heavily pretreated relapsed and refractory MM patients, even as a single agent *(13)*. However, not all of the heavily pre-treated patients respond to single agent daratumumab and some patients who initially respond progress eventually *(14)*. Therefore, there is a need for a companion diagnostic to stratify patients who will benefit from the daratumumab therapy. Antibody based imaging agents are playing an ever more important role in the clinic as demonstrated by trastuzumab and pertuzumab bioconjugates for the human epidermal growth factor receptor 2 (HER2) imaging *(15)*.

In this study, we evaluated daratumumab for PET/CT imaging of MM. The proof-of-principle *in vitro* and *in vivo* data in the CD38$^+$ human myeloma cells and MM mouse models demonstrate the potential of daratumumab-based imaging agents for stratifying patients for daratumumab therapy. Specific antibodies such as daratumumab are also attractive platforms for targeted alpha-particle radiation therapy *(16, 17)*.

We hypothesize that the enhanced specific expression of CD38 glycoprotein on malignant plasma cells will favor increased [89Zr]Zr-DFO-daratumumab uptake and allow for clinically impactful PET imaging for therapeutic planning as a companion diagnostic. The goal of this project is to develop and validate daratumumab-based imaging agents that will eventually help stratify patients for

daratumumab therapy, minimizing off-target toxicities and reduce unnecessary treatment of patients not likely to respond. The safety profile and targeting efficacy of daratumumab render it an ideal candidate for radiation therapy as well in future studies. These studies will contribute toward technological advancements in diagnostic and therapeutic monoclonal antibody based radiopharmaceutical development for MM and lymphoid tumors in general.

MATERIALS AND METHODS:

Ethics statement

All experiments involving the use of radioactive materials at Washington University were conducted under the authorization of the Radiation safety Commission in accordance with the University's Nuclear Regulatory commission license. All animal studies were performed under the guide for the Care and Use of Laboratory Animals under the auspices of the Washington University Animal Studies Committee. The data in any tables and any radiation or radiopharmaceutical doses mentioned are verified and correct.

Synthesis and characterization of daratumumab-DFO

For the synthesis of the daratumumab-DFO conjugate, daratumumab (20 mg/mL; 0.012 µmoles) was incubated with DFO-Bz-NCS (0.18 µmoles) using 0.1M sodium carbonate (pH=9) as the conjugating buffer. The reaction mixture was incubated at 37 °C for 1 h. Chelator was conjugated to the antibody *via* a thiourea linkage, and the conjugate was purified using Zeba spin columns (M_w cut off = 40 kDa, 0.5 mL; Thermo Fisher Scientific, Rockford, IL). The protein concentration of resultant DFO functionalized antibody was determined by bicinchoninic acid assay (Thermo Fisher Scientific, Rockford, IL). Conjugation efficiency was evaluated by ESI-MS (Supplemental Fig. 1A).

Radiolabeling of daratumumab-DFO with Zr-89

Daratumumab-DFO conjugate was added to neutralized [89Zr]Zr-oxalate, and the reaction mixture was incubated at 37 °C for 1 h while shaking. Radiochemical purity was determined by instant thin-layer chromatography using 50mM diethylenetriaminepentaacetic acid as the mobile phase. The serum stability of the radiolabeled antibody was determined at four different time intervals (1, 2, 3 and 7 days) (Supplemental Fig. 1B).

Flow cytometry, *in vitro* saturation binding assay, *in vitro* cell uptake and immunoreactivity assay

Details are provided in the supplemental file.

Synthesis of daratumumab-Cy5

A freshly prepared 10 µL aliquot of Sulfo-Cyanine5 (Cy5) NHS ester (1 mg/mL in water) was added to 100 µL of daratumumab (20 mg/mL) and the total volume was adjusted to 200 µL using 0.1 M sodium carbonate buffer (pH-9). The Cy5 dye was added to daratumumab solution at a 5:1 molar ratio and the reaction mixture was incubated at 37 °C for 2 h with gentle shaking. Details are provided in the supplemental file.

Confocal microscopy

MM1.S cells were plated on 35 mm glass bottom dishes coated with polylysine (MatTek Corporation, glass no. 1.5), and incubated for an hour at 37 °C, 5% CO_2 to let cells attach to the glass surface. To test binding to cell surface CD38, attached cells were treated with daratumumab-Cy5 (14 mg/mL, 1µM with respect to Cy5) and Hoechst 33342 (10 µg/mL) for 10 minutes at 4 °C with or without 100-fold molar excess of unlabeled daratumumab as a blocking agent. Details are provided in the supplemental file.

Tissue distribution of ^{89}Zr-daratumumab in MM1.S tumor-bearing mice

Tissue biodistribution studies were performed to evaluate the uptake of [89Zr]Zr-DFO-daratumumab in normal (n = 4) and MM1.S tumor-bearing SCID mice (n = 6). Bioluminsecence imaging was performed to confirm tumor location and estimate tumor burden. Prior to tissue biodistribution studies, mice were injected *via* lateral tail vein with 100 µL of 1.11 MBq [89Zr]Zr-DFO-daratumumab (Specific Activity: 55.5 MBq/nmole) in saline. Blocking studies were conducted with 200-fold molar excess of cold daratumumab (100 µL) injected *via* lateral tail vein at 15 min prior to the injection of [89Zr]Zr-DFO-daratumumab (1.11 MBq) in mice. Details are provided in the supplemental file.

Small animal [89]Zr-daratumumab-PET/CT imaging

Small animal [89Zr]Zr-DFO-daratumumab-PET/CT imaging was conducted in Fox Chase SCID beige mice bearing MM1.S subcutaneous and disseminated myeloma tumors. Prior to small animal PET/CT imaging, mice were injected via lateral tail vein with [89Zr]Zr-DFO-daratumumab (1.11MBq). Details are provided in the supplemental file.

Data analysis and Statistics

All data are presented as mean ± standard deviation. Groups were compared using Prism 5.0 (GraphPad Software, Inc., CA). P values of less than 0.05 were considered statistically significant.

RESULTS

Synthesis and characterization of daratumumab-DFO

The anti-CD38 antibody, daratumumab, was modified with the bifunctional chelator DFO-Bz-NCS with a 15:1 molar excess of chelator to the antibody. Based on the ESI mass spectra, the calculated average number of chelators attached to single antibody molecule was approximately 7 (Supplemental Fig. 1A).

Radiolabeling and stability of radiolabeled daratumumab-DFO

Daratumumab-DFO was radiolabeled using neutralized [89Zr]Zr-oxalate resulting in the specific activity of 55.5 MBq/nmole. High radiochemical purity (>99%) was obtained after the labeled conjugate was purified using Zeba spin columns. The crude and purified compound was evaluated by radio-thin layer chromatograhy using 50mM diethylenetriaminepentaacetic acid as the mobile phase (Supplemental Fig. 1B). *In vitro* serum stability tests demonstrated that the radiolabeled antibody was stable with > 98% intact radioactivity with the antibody for up to 7 days (Supplemental Fig. 1C).

Flow Cytometry

For the proof-of-principle *in vitro* and *in vivo* studies a CD38 expressing myeloma cell line was desirable. The human MM cell line MM1.S was derived from a biopsy sample from a 42 year old African American woman and is commonly used for evaluating therapies in preclinical studies *(18)*. Flow cytometry studies using MM1.S human myeloma cell line confirmed the high expression of CD 38 antigen (>99% of cells staining positive) and therefore, was utilized for cellular and *in vivo* studies (Fig. 1A). Flow cytometry additionally confirmed that the expression CD38 on MM1.S cells remained intact after inoculation into SCID mice (Supplemental Fig. 2).

***In vitro* saturation binding, cell uptake and immunoreactivity assay**

[89]Zr-daratumumab demonstrated saturable binding to CD38^{+} MM1.S human myeloma whole cells. The concentration at which the radiolabeled antibody occupied 50% of the cell surface receptors (K_d) was determined to be 3.3 nM (± 0.58). A representative saturation binding curve and Scatchard transformation of [89Zr]Zr-DFO-daratumumab binding to MM1.S cells is shown in Fig. 1B. The data demonstrated that in the concentration range of 0.25 – 16.0 nM, [89Zr]Zr-DFO-daratumumab is bound to a single class of binding sites with a B_{max} of 10.1 fmoles/mg (± 0.64). Additionally, whole cell uptake (sum of the cell internalized and cell surface bound fractions at 37 °C) for [89Zr]Zr-DFO-daratumumab in MM1.S cells in the presence and absence of the blocking

agent (cold daratumumab) was significantly reduced (P < 0.0001) (Fig. 1C). The immunoreactive fraction determined using Lindmo assay was 95% (Supplemental Fig. 3).

Confocal microscopy with daratumumab-cy5

The sulfo-Cy5-NHS ester optical dye (5 equivalents) was successfully coupled to 1 equivalent of daratumumab, and the conjugates were characterized qualitatively by gel electrophoresis (Supplemental Fig.4). Gel electrophoresis results showed that the conjugation did not alter the fluorescence characteristics of the optical dye, and the excitation (646 nm) and emission (662 nm) spectra of the daratumumab-Cy5 conjugate were similar to that of free dye. The binding of daratumumab-Cy5 was evaluated in MM1.S cells using confocal microscopy. MM1.S cells were treated with daratumumab-Cy5 in the absence and presence of a 100-fold molar excess of unlabeled daratumumab. Confocal laser scanning microscopy images showed that MM1.S cells in the absence of block efficiently bound the fluorescent-antibody conjugate when compared to the cells in the presence of blocking, demonstrating the binding specificity of the conjugate (Fig. 2).

Small animal PET/CT imaging

Fox Chase SCID beige mice bearing MM1.S subcutaneous tumor xenografts when injected intravenously with [89Zr]Zr-DFO-daratumumab demonstrated significant tumor-selective uptake. Small animal PET images of these mice showed that the radiolabeled bioconjugate had appropriate sensitivity and selectivity for detecting myeloma tumors of different sizes and heterogeneity, as even early stage non-palpable, tumor lesions were clearly visible in the PET images (Fig. 3A). Regions of interest analysis of PET images demonstrated that the standard uptake values ranged from 2.1 to 9.3 in tumors of different sizes and volumes (8.5 to 128 mm^3) (Figs. 3A and 3B). [89Zr]Zr-DFO-daratumumab uptake was significantly reduced in the presence of a 200-fold molar excess of the cold antibody as shown in the PET image (Fig. 4A). The auto-

radiographic slices from excised tumors are in concert with the PET/CT imaging data, with reduced radioactivity in the blocked tumor (Fig. 4C). Representative bioluminescence and CT images of the mouse used in the blocking study confirmed the presence of tumor on the right flank (Figs. 4B and 4D). The CD38 expression is retained (>99%) in the engrafted MM1.S tumors as verified independently by flow cytometry (Supplemental Fig. 2). The specificity was further demonstrated in CD38^{low} murine MM 5TGM1 cells, where the established intra-tibial 5TGM1 tumors did not specifically retain [89Zr]Zr-DFO-daratumumab as shown in Supplemental Fig. 5.

To demonstrate the *in vivo* imaging of skeletal tumor lesions, [89Zr]Zr-DFO-daratumumab PET/CT was performed in a MM1.S disseminated MM mouse model (n=4). The representative bioluminescence image (Fig. 5A) validated the tumor presence in the bone marrow rich skeletal sites such as femur, tibia and the spinal cord. Mice with MM1.S disseminated tumors were imaged at 7 days post administration of [89Zr]Zr-DFO-daratumumab. The small animal PET/CT images demonstrated significant radiotracer uptake in the tumor-bearing lesions. The representative images of the disseminated mouse model and the corresponding tumor-free SCID mouse are shown in Fig. 5B.

Tissue distribution of [89Zr]Zr-DFO-daratumumab in wild-type and tumor bearing MM mice

Tissue biodistribution studies were performed in the wild-type and subcutaneous MM1.S tumor-bearing SCID mice using [89Zr]Zr-DFO-daratumumab at 6 and 7 days post administration of the radiopharmaceutical. Biodistribution studies in a disseminated tumor model are challenging as the bones are rendered fragile due to myeloma induced lysis. The biodistribution data in the subcutaneous tumor mice were in agreement with the PET imaging data showing considerably high uptake and retention in tumor tissue at 7 days post injection with the uptake of 27.7 ± 7.6 %ID/g (Fig. 6). High concentration of radioactivity was seen in the spleen with 31.5 ± 7.5 %ID/g, as previously observed with [89Zr]Zr-DFO-labeled antibodies *in vivo (19, 20)*. The %ID/g in remaining normal tissues was significantly lower than the tumor tissues. The [89Zr]Zr-DFO-

daratumumab tissue biodistribution in non-tumor-SCID mice showed the expected trend with highest %ID/g retention in spleen (25.6 ± 3.4) (Supplemental Table 1).

A separate set of mice was used to perform blocking studies to evaluate the specificity of [89Zr]Zr-DFO-daratumumab *in vivo* in the MM1.S xenograft subcutaneous mouse model. In the blocking group, splenic uptake (31.5 ± 6.1 *versus* 10.6 ± 1.4) and tumor associated activity was significantly reduced (~3-fold decrease) when compared to the non-blocked tumor. The blocking study did not significantly alter the uptake in other non-tumor tissues (Supplemental Table 2).

DISCUSSION

High expression of CD38 antigen on malignant plasma cells complemented with a relatively low expression on normal lymphoid and myeloid cells make it a desirable therapeutic target *(10)*. Approved by US Food and Drug Administration in 2016, daratumumab is a therapeutic human monoclonal antibody with high affinity for the unique CD38 epitope. Daratumumab has demonstrated favorable safety profile and efficacy as monotherapy and in combination with other drugs in pretreated relapsed and refractory myeloma patients *(13)*. Pre-clinical studies published by Tai et al. suggested that daratumumab effectively killed primary CD38$^+$ and CD138$^+$ patient MM cells and a range of MM cell lines by antibody-dependent cellular and complement dependent cytotoxicity mechanisms *(21)*. While promising clinically, not all patients respond to daratumumab monotherapy, highlighting the need for patient stratification for daratumumab therapy. Additionally, an effective strategy to identify responsive from non-responsive phenotypes will help understand the mechanisms of resistance and eventually lead to methods for overcoming resistance through sensitization to therapy.

Antibodies have evolved as reliable vehicles for the delivery of radionuclides and drugs to cancer cells due to their sensitivity, selectivity, and affinity. Radiolabeled antibody-based agents directed toward tumor-associated antigens can be used to evaluate the specific uptake by cancer

molecular biomarkers. Antibody-based imaging agents are making a positive impact in the clinic by helping to stratify patients for targeted therapies and monitoring therapy responses based on the level of tumor associated antigen expression *(22-24)*.

Zr-89 is a desirable and validated long-lived PET radionuclide with a half-life of 3.3 d that matches the slow pharmacokinetics of the intact antibodies *(25)*. The DFO ligand coordinates Zr^{4+} easily at room temperature, is stable in human serum for up to seven days, and PET images have demonstrated excellent spatial resolution and signal to noise ratios in human patients *(26)*. Human radiation dosimetry of [89Zr]Zr-DFO-trastuzumab in patients with HER2 positive breast cancer showed that it is safe for human applications *(27,28)*. There are currently over twenty ongoing clinical trials to evaluate antibody-based imaging agents for imaging and treating different solid and hematological cancers *(29)*. Moreover, these clinical studies are geared to image the expression of proteins that would benefit from targeted therapy, evaluate treatment response, and detect recurrent cancers *(30)*.

A sensitive, non-invasive functional PET imaging probe is highly desirable to evaluate the expression of CD38 in myeloma cells for therapy planning of MM. Targeted molecular imaging approaches could also help in differentiating MM from other monoclonal plasma cell malignancies *(31, 32)*. Therefore, we have evaluated the efficacy of [89Zr]Zr-DFO-daratumumab to image CD38⁺ expression in mouse models of MM. We demonstrated that DFO-daratumumab could be stably and reproducibly labeled with Zr-89 while preserving the antigen binding capacity. [89Zr]Zr-DFO-daratumumab demonstrated high affinity for the human myeloma cell line MM1.S *in vitro* and *in vivo*. CD38⁺ click beetle red transfected MM1.S human myeloma cells were utilized for *in vitro* and *in vivo* proof-of-principle studies for evaluating [89Zr]Zr-DFO-daratumumab. Flow cytometry and cell uptake assays confirmed high expression of CD38 on MM1.S cells *in vitro* and *ex vivo*. The cell uptake and saturation binding assays showed that [89Zr]Zr-DFO-daratumumab

can bind with high affinity and specificity to CD38$^+$ myeloma cells. Importantly, the immunoreactivity of [89Zr]Zr-DFO-daratumumab was determined to be > 95%.

Preclinical PET/CT imaging with [89Zr]Zr-DFO-daratumumab was supported by *in vitro* cell binding and uptake studies, fluorescence confocal microscopy, *ex vivo* biodistribution and autoradiography of the tumor slices. *Ex vivo* tissue biodistribution data demonstrated that ^{89}Zr-daratumumab had specific uptake in MM1.S myeloma tumors 6 and 7 days post administration of the radiopharmaceutical. The tumor uptake was considerably reduced in the presence of excess unlabeled daratumumab, demonstrating specificity and affinity of the monoclonal antibody for CD38$^+$ cells *in vivo*. The CD38^{low} murine 5TGM1 cells had significantly lower uptake of [89Zr]Zr-DFO-daratumumab in cells and *in vivo*.

PET imaging performed at 6 and 7 days post administration of [89Zr]Zr-DFO-daratumumab in mice bearing subcutaneous MM tumors showed high radiotracer uptake in tumors of variable sizes with a superb tumor to background contrast. Furthermore, PET images in the disseminated mouse model showed that the tumor cells localized in femur, tibia, and spine were readily detectable by [89Zr]Zr-DFO-daratumumab. The CD38^{low} murine 5TGM1 MM tumors did not retain [89Zr]Zr-DFO-daratumumab *in vivo* further highlighting specificity. As previously shown in mice, relatively high uptake occurred in the spleen and bone. In organs such as the spleen, blood capillaries have sinusoidal clefts of about 100 nm allowing monoclonal antibodies to freely travel through these clefts, explaining the splenic uptake *(33)*. Previous studies have shown elevated levels of ^{89}Zr in the remodeling bones of mice injected with [89Zr]Zr-DFO-labeled antibodies, attributed to metabolism of osteophilic ^{89}Zr^{4+} from the ligand *in vivo* by less selective mouse liver enzymes *(34,35)*. Human studies with [89Zr]Zr-DFO-labeled antibodies have however shown minimal uptake in bone *(36)*. Thus, our preclinical data demonstrate that [89Zr]Zr-DFO-daratumumab is a promising antibody based PET radiopharmaceutical for non-invasive imaging of CD38$^+$ myeloma tumors.

CONCLUSION

We have developed daratumumab-based PET and optical imaging probes that specifically target CD38 antigen and can be used to image CD38$^+$ tumors with high specificity. These studies demonstrate the potential of [89Zr]Zr-DFO-daratumumab as a PET molecular imaging agent for MM for diagnosis, patient stratification and long-term follow-up.

ACKNOWLEDGEMENTS

REFERENCES

1.   Kuehl WM, Bergsagel PL. Multiple myeloma: evolving genetic events and host interactions. *Nat Rev Cancer.* 2002;2:175-187.

2.   Kuehl WM, Bergsagel PL. Molecular pathogenesis of multiple myeloma and its premalignant precursor. *J Clin Invest.* 2012;122:3456-3463.

3.   Kyle RA, Gertz MA, Witzig TE, et al. Review of 1027 Patients With Newly Diagnosed Multiple Myeloma. *Mayo Clin Proc.* 2003;78:21-33.

4.   Kumar SK, Rajkumar SV, Dispenzieri A, et al. Improved survival in multiple myeloma and the impact of novel therapies. *Blood.* 2008;111:2516-2520.

5.   Tai YT, Anderson KC. Antibody-based therapies in multiple myeloma. *Bone Marrow Res.* 2011;2011:924058.

6.   Parren PW, van de Winkel JG. An integrated science-based approach to drug development. *Curr Opin Immunol.* 2008;20:426-430.

7.   Malavasi F, Deaglio S, Damle R et al. CD38 and chronic lymphocytic leukemia: a decade later. *Blood.* 2011;118:3470-3478.

8.   Deaglio S, Mehta K, Malavasi F. Human CD38: a (r)evolutionary story of enzymes and receptors. *Leuk Res.* 2001;25:1-12.

9.   van de Donk N.W, Janmaat ML, Mutis T, et al. Monoclonal antibodies targeting CD 38 in hematological malignancies and beyond. Immunol Rev. 2016; 270: 95–112.

10.   Stevenson GT. CD 38 as a therapeutic target. *Mol Med.* 2006;12:345-346.

11.   McKeage K. Daratumumab: First Global Approval. *Drugs.* 2016;76:275-281.

12.   de Weers M, Tai YT, van der Veer MS, et al. Daratumumab, a novel therapeutic human CD38 monoclonal antibody, induces killing of multiple myeloma and other hematological tumors. *J Immunol.* 2011;186:1840-1848.

13.   Phipps C, Chen Y, Gopalakrishnan S, et al. Daratumumab and its potential in the treatment of multiple myeloma: overview of the preclinical and clinical development. *Ther Adv Hematol.* 2015;6:120-127.

14.   Nijhof IS, Casneuf T, van Velzen J, et al. CD38 expression and complement inhibitors affect response and resistance to daratumumab therapy in myeloma. *Blood.* 2016;128:959-970.

15.   Wang RE, Zhang Y, Tian L, et al. Antibody-based imaging of HER-2: moving into the clinic. *Curr Mol Med.* 2013;13:1523-1537.

16. Maguire WF, McDevitt MR, Smith-Jones PM et al. Efficient 1-Step Radiolabeling of Monoclonal Antibodies to High Specific Activity with Ac-225 for alpha-Particle Radioimmunotherapy of Cancer. *J Nucl Med.* 2014;55:1492-1498.

17. Jurcic JG, Larson SM, Sgouros G, et al. Targeted at particle immunotherapy for myeloid leukemia. *Blood.* 2002;100:1233-1239.

18. Greenstein S, Krett NL, Kurosawa Y, et al. Characterization of the MM.1 human multiple myeloma (MM) cell lines: a model system to elucidate the characteristics, behavior, and signaling of steroid-sensitive and -resistant MM cells. *Exp Hematol.* 2003;31:271-282.

19. Nagengast WB, de Vries EG, Hospers GA, et al. In vivo VEGF imaging with radiolabeled bevacizumab in a human ovarian tumor xenograft. *J Nucl Med.* 2007;48:1313-1319.

20. Marquez BV, Ikotun OF, Zheleznyak A, et al. Evaluation of (89)Zr-pertuzumab in Breast cancer xenografts. *Mol Pharm.* 2014;11:3988-3995.

21. Tai YT, de Weers M, Li XF, et al. Daratumumab, a novel potent human anti CD 38 monoclonal antibody, induces significant killing of human multiple myeloma cells: Therapeutic Implication. *ASH Annu Meet Abstr.* 2009;114:608.

22. Van de Watering FC, Perk L, Brinkmann U, et al . Zirconium-89 Labeled Antibodies: A New Tool for Molecular Imaging in Cancer Patients. *BioMed Res Int.* 2014;203601. doi:10.1155/2014/203601.

23. Muselaers CH, Stillebroer AB, Desar IM, et al. Tyrosine kinase inhibitor sorafenib decreases 111In-girentuximab uptake in patients with clear cell renal cell carcinoma. *J Nucl Med.* 2014;55:242-247.

24. van Dongen GA, Visser GW, Lub-de Hooge MN, et al. Immuno-PET: a navigator in monoclonal antibody development and applications. O*ncologist.* 2007;12:1379-1389.

25. Zeglis BM, Lewis JS. The bioconjugation and radiosynthesis of 89Zr-DFO-labeled antibodies. *J Vis Exp.* 2015; 96: 52521.

26. Wang RE, Zhang Y, Tian L, et al. Antibody-based imaging of HER-2: moving into the clinic. *Curr Mol Med.* 2013;13:1523-1537.

27. Laforest R, Lapi SE, Oyama R, et al. [89Zr]Trastuzumab: Evaluation of Radiation Dosimetry, Safety, and Optimal Imaging Parameters in Women with HER2-Positive Breast Cancer. *Mol Imaging Biol.* 2016;18:952-959.

28. Borjesson PK, Jauw YW, de Bree R, et al. Radiation dosimetry of 89Zr-labeled chimeric monoclonal antibody U36 as used for immuno-PET in head and neck cancer patients. *J Nucl Med.* 2009;50:1828-1836.

29. Sliwkowski MX, Mellman I. Antibody therapeutics in cancer. *Science.* 2013;341:1192-1198.

30.   Warram JM, de Boer E, Sorace AG, et al. Antibody-based imaging strategies for cancer. *Cancer Metastasis Rev.* 2014;33:809-822.

31.   Vij R, Fowler KJ, Shokeen M. New Approaches to Molecular Imaging of Multiple Myeloma. *J Nucl Med.* 2016;57:1-4.

32.   Lemaire M, D'Huyvetter M, Lahoutte T, et al. Imaging and radioimmunotherapy of multiple myeloma with anti-idiotypic Nanobodies. *Leukemia.* 2014;28:444-447.

33.   Tabrizi M, Bornstein GG, Suria H. Biodistribution mechanisms of therapeutic monoclonal antibodies in health and disease. *AAPS J.* 2010;12:33-43.

34.   Abou DS. *In vivo* biodistribution and accumulation of 89Zr in mice. *Nucl Med Biol.* 2011;38(5):675-81.

35.   Terwisscha van Scheltinga AG, Ogasawara A, Pacheco G, et al. Preclinical Efficacy of an Antibody-Drug Conjugate Targeting Mesothelin Correlates with Quantitative 89Zr-ImmunoPET. *Mol Cancer Ther.* 2017;16:134-142.

36.   Dijkers EC, Oude Munnink TH, Kosterink JG, et al. Biodistribution of 89Zr-trastuzumab and PET imaging of HER2-positive lesions in patients with metastatic breast cancer. *Clin Pharmacol Ther.* 2010;87:586-592.
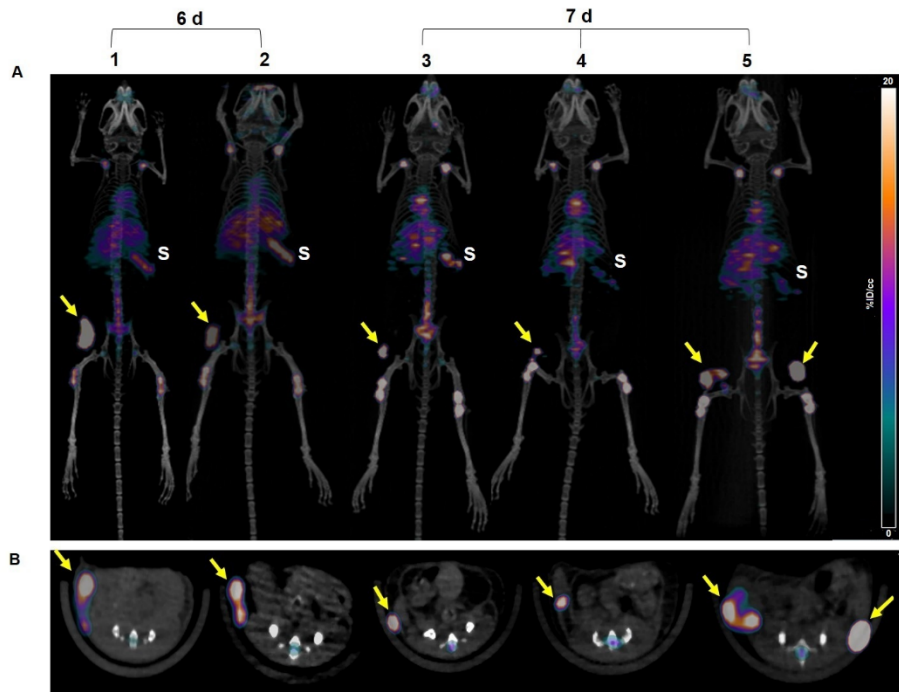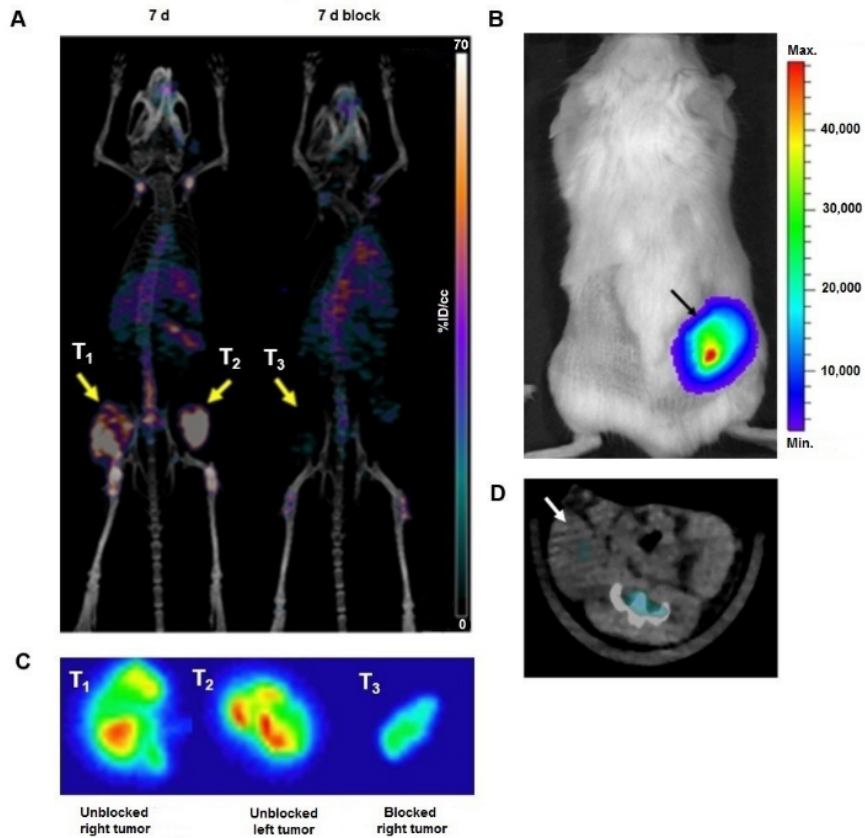
FIGURES
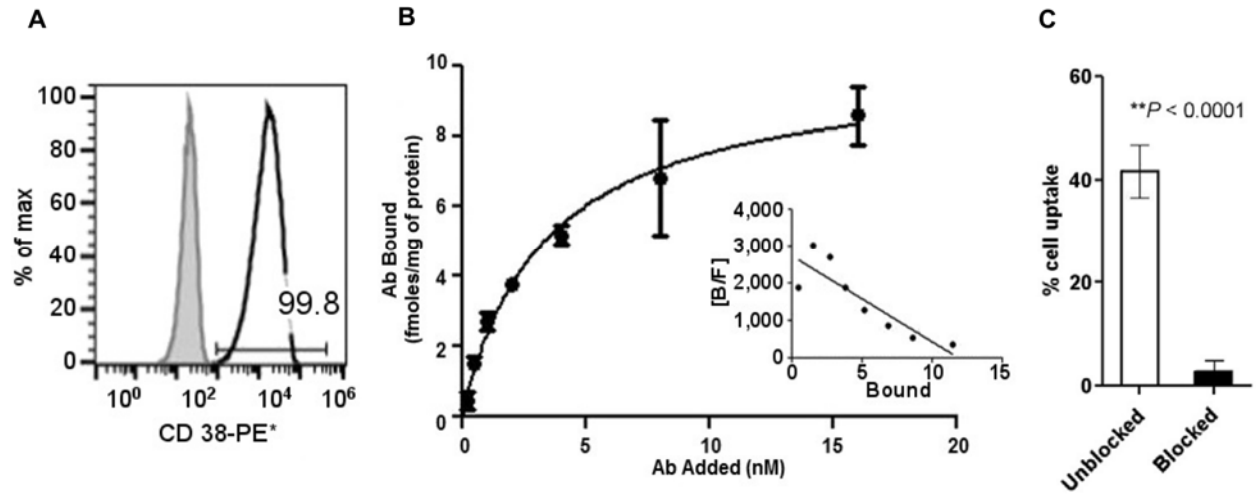
FIGURE 1. (A) Flow cytometry data validated >99% CD38⁺ expression as compared to the isotype control in the human MM1.S myeloma cells (PE=Phycoerythrin), (B) Saturation binding curve for [89Zr]Zr-DFO-daratumumab in MM1.S cells; n=3 (Inset: Scatchard transformation of saturation binding data), (C) % cell uptake for [89Zr]Zr-DFO-daratumumab in MM1.S cells at 37 °C in the absence and presence of 200-fold blocking dose of cold daratumumab.

Cy 5 Nucleus GFP
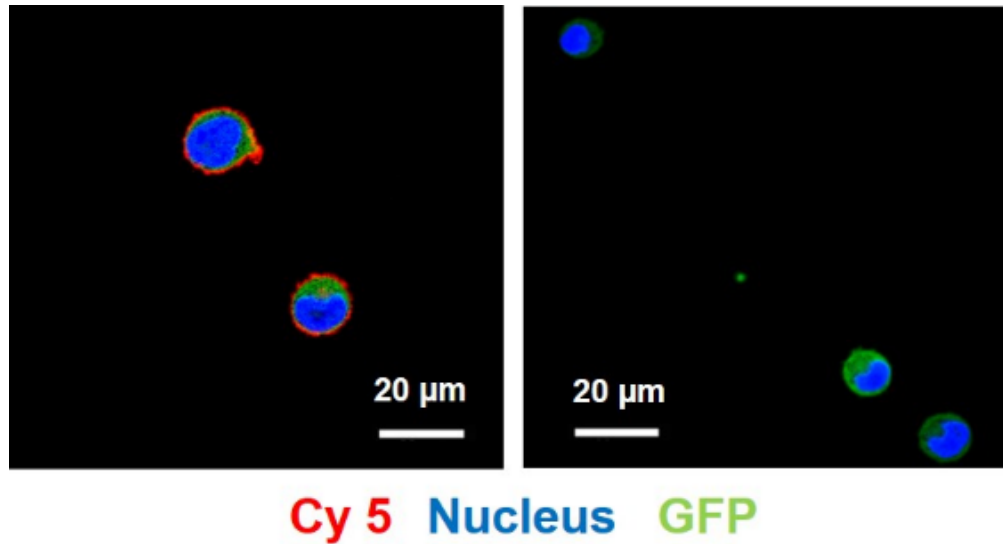
FIGURE 2. (a) Confocal microscopy images of MM1.S cells treated with daratumumab-Cy5 showed strong cell surface signal; Red: Cy5, Green: GFP, Blue: Hoechst 33342 (nuclear co-stain). (b) Cell surface binding is significantly reduced in the presence of 100-fold molar excess of unlabeled anti-CD38 antibody as blocking agent. Scale bar represents 20 μm.

FIGURE 3. (A) Representative maximum intensity projection (MIP) coronal [89Zr]Zr-DFO-daratumumab-PET/CT images in MM1.S subcutaneous tumor bearing SCID mice at 6 days (n=2) and 7 days (n=3) post injection of the radiopharmaceutical. S=Spleen. (B) Axial planes corresponding to images shown in panel **A**. Non-palpable and palpable tumors with volumes ranging from 8.47 to 128.1 mm^3 showed efficient tracer uptake (Tumors=Yellow arrows).

FIGURE 4. (A) Left-Representative MIP [89Zr]Zr-DFO-daratumumab/PET/CT image of mouse with bi-lateral subcutaneous MM1.S tumors (T_1 and T_2) in the absence of blocking agent; Right-[89Zr]Zr-DFO-daratumumab/PET/CT image of a mouse with unilateral subcutaneous MM1.S tumor (T_3) that received 200-fold molar excess of cold daratumumab as a blocking agent. Both mice were imaged at 7 days post injection of [89Zr]Zr-DFO-daratumumab.

(B) Representative bioluminescence image of the subcutaneous MM1.S tumor (T_3) bearing mouse used for blocking study demonstrating the extent of tumor progression (black arrow). Bioluminescence Scale: Photon Counts

(C) Representative autoradiography images of frozen tumor slices showing distribution of [89Zr]Zr-DFO-daratumumab within the imaged MM1.S tumors (T_1, T_2, T_3).

(D) Axial CT image of the mouse used in the blocking study. The subcutaneous tumor (white arrow) is confirmed in the bioluminescence image.
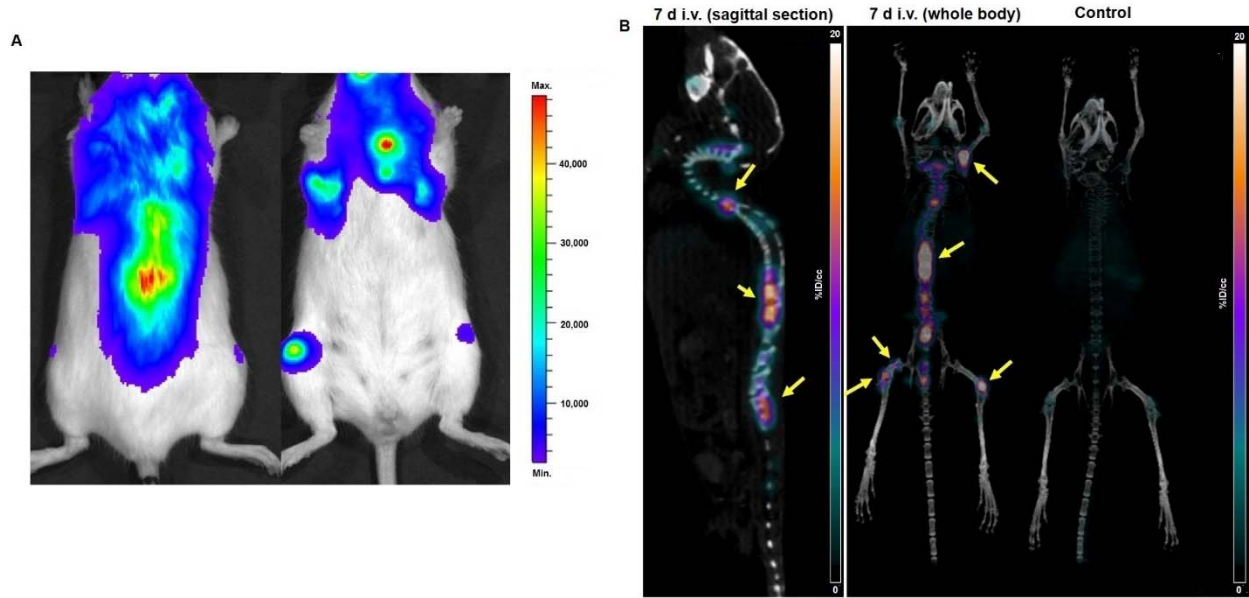
FIGURE 5. (A) Representative bioluminescence image of the mouse in prone and supine position demonstrating the extent of tumor progression in the disseminated MM1.S tumor model. Bioluminescence Scale: Photon Counts, (B) [89Zr]Zr-DFO-daratumumab-PET/CT image (sagittal and coronal views) of the disseminated MM1.S tumor-bearing mouse and a non-tumor control mouse.
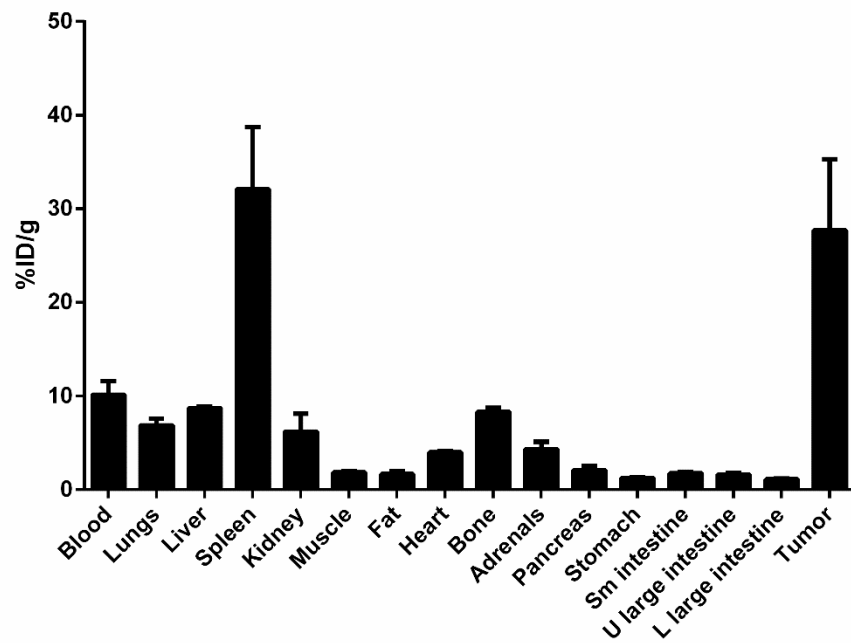
FIGURE 6. Biodistribution of [89Zr]Zr-DFO-dararumumab in human MM1.S subcutaneous Xenografts (n=3) at 7 days post administration of the radiotracer.

MATERIALS

All chemicals were purchased in the highest available purity, and solutions were prepared using ultrapure water (18 MΩ-cm resistivity, Millipore system). Daratumumab was provided by the Siteman Cancer Center pharmacy, St Louis, MO. DFO-Bz-NCS was purchased from Macrocyclics, Inc. (Dallas, TX). The optical dye, Sulfo-Cy5 NHS ester was purchased from Lumiprobe Corporation (Hallandale Beach, FL). All other chemicals used in the conjugation, radiolabeling and purification steps were purchased from Sigma Aldrich (St Louis, MO). ESI-MS were obtained using Thermo Exactive EMR (Thermo Fisher Scientific, Rockford, IL) at the Washington University Mass Spectrometry Core Facility. Zr-89 was produced *via* the ^{89}Y (p, n) ^{89}Zr reaction on a CS-15 cyclotron (Cyclotron corporation, Berkeley, CA) at Washington University Cyclotron Facility. Information on cell lines and animal models is provided in the supplemental file.

METHODS

Synthesis and characterization of daratumumab-DFO

A stock solution of DFO-Bz-NCS (5 mg/mL) was prepared in DMSO. To the antibody, 15-fold molar excess of DFO chelator (0.18 µmoles) and the conjugating buffer (0.1 M sodium carbonate buffer; pH-9) was added to bring the reaction volume to 200 µL. The reaction mixture was incubated at 37 °C for 1 h. Daratumumab-DFO conjugate was purified from the unreacted DFO by size exclusion chromatography using desalting Zeba spin columns (M_w cut off = 40 kDa, 0.5 mL; Thermo Fisher Scientific, Rockford, IL).

To confirm the degree of conjugation, mass spectral analysis of the unmodified antibody (daratumumab) and the daratumumab-DFO conjugate, ESI-MS was performed (Supplemental Figure 1A). An average number of DFO molecules attached to the mAb were calculated by using the following formula:

$$number\ of\ DFO\ molecules\ conjugated$$

$$= \frac{increase\ in\ molecular\ weight\ relative\ to\ unmodified\ antibody}{molecular\ weight\ of\ DFO}$$

Radiolabeling of daratumumab-DFO conjugate

For radiolabeling, 1-5 mCi of [89]Zr-oxalate solution (pH<1) was neutralized to pH 6.2-7.1 by adding an equivalent volume of 0.1 M HEPES buffer (pH-7) followed by slow addition of 2 M sodium hydroxide. Further, DFO functionalized antibody was incubated with [89]Zr at 37 °C for 1 h. The reaction mixture was challenged with 5-10 µL of 50mM diethylenetriaminepentaacetic acid (DTPA) to assay for unreacted or non-specifically bound [89]Zr. Labeling efficiency was determined by iTLC using 50 mM DTPA as the mobile phase (Supplemental Figure 1B).

The serum stability of the radiolabeled antibody was evaluated by incubating 0.1 mL of the radiolabeled complex with 0.9 mL of human serum at 37 °C. The radiochemical purity was determined by iTLC using 50 mM diethylenetriaminepentaacetic acid as the mobile phase at incubation intervals of 1, 2, 3, and 7 days (Supplemental Figure 1C).

Cell lines

The human multiple myeloma cancer cell line (MM1.S), a commonly used cell line to evaluate novel therapies for MM was obtained from DiPersio Laboratory (Professor John F. DiPersio, Department of Medicine, Washington University School of Medicine, St Louis, USA). The cells were cultured in Roswell Park Memorial Institute (RPMI) 1640 medium (Thermo Fischer Scientific) supplemented with 10% heat inactivated fetal bovine serum (FBS) and 1% Streptomycin. All these cells were maintained at 37 °C in 5% CO_2 and 90% humidity.

Murine multiple myeloma cancer cell line (5TGM1-GFP-*luc*) was obtained from Professor Katherine N Weilbaecher (Department of Medicine, Oncology Division, Washington University School of Medicine, St Louis, USA). These cell lines were cultured in Iscove's Modified Dulbecco's

(IMDM) medium (Thermo Fischer Scientific) supplemented with 10% heat inactivated fetal bovine serum (FBS) and 1% Streptomycin. All these cells were maintained at 37 °C in 5% CO_2 and 90% humidity.

Flow cytometry

The human myeloma MM1.S and murine myeloma 5TGM1 cells were grown and analyzed for CD38 antigen expression by flow cytometry. Phycoerythrin (PE) conjugated anti-human CD38 antibody (HB7, Abcam Biotechnology) was used to evaluate CD38 expression on the MM1.S cells. BV421 Rat Anti-Mouse CD38 Clone 90/CD38 (also known as Ab90) (Fischer scientific) was used for alalyzing CD38 expression on the 5TGM1 cells. For cell surface staining, MM1.S cells or 5TGM1 cells (2×10^5) were prepared in 100 µL of buffer, phosphate buffered saline containing 0.1% bovine serum albumin (BSA). Cells were incubated with phycoerythrin conjugated anti-CD38 antibody or isotype control antibody (MOPC-21, BD biosciences) for 30 min at 4 °C in dark. After incubation, cells were washed twice with buffer. MM1.S cells were stained with 7-amino-actinomycin D for dead cell exclusion for 5 minutes and analyzed on a Beckman Coulter Gallios flow cytometer. Data were analyzed using FlowJo software (TreeStar, Ashland, OR).

MM1.S MM mouse models

Fox Chase Beige mice (Charles River Laboratories) were housed in ventilated cage racks and allowed food and water. Mice were injected with MM1.S cells (10^6 cells) with matrigel in the flank either unilaterally or bi-laterally. The tumors were allowed to grow for ~7-10 days. For the disseminated mouse model, mice were injected i.v. by tail vein with MM1.S tumor cells in PBS (10^6 cells/100 µL) or only PBS for vehicle control.

Murine 5TGM1-GFP-*Luc* in C57Bl/KaLwRij multiple myeloma (MM) model

A localized, intratibial tumor model was generated by inoculating 5TGM1-GFP-luc cells (200,000 cells in 25uL 1x PBS) into one of the tibias of C57Bl/KaLwRij mice, with a contralateral injection of saline as an inflammation control.

In vitro Saturation binding assay

The dissociation constant (K_d) and receptor density (B_{max}) for [89Zr]Zr-DFO-daratumumab was measured using the radioligand saturation receptor binding assay. For saturation binding experiments, [89Zr]Zr-DFO-daratumumab (0.25 – 32 nM) was incubated with 2.5 x10^6 MMI.S cells for 3 h at 4 °C with slight shaking. After the incubation, the samples were centrifuged at 1500 rpm for 5 min, the supernatant was removed by vacuum aspiration and the cells were washed twice with ice cold phosphate buffered saline (PBS) to remove the unbound radioactivity. Non-specific binding was determined by performing the assay in the presence of (200-fold) excess of unlabeled daratumumab. The radioactivity in cell pellets was measured using a gamma counter. The specific binding was obtained by subtracting the non-specific binding from total binding. The dissociation constant (K_d) and receptor density (B_{max}) were estimated form the non-linear fitting of the specific binding versus the concentration of [89Zr]Zr-DFO-daratumumab using Prism software (Graph Pad, San Diego, CA).

In vitro cell uptake assay

Cell uptake studies were performed in the MM1.S cells using [89Zr]Zr-DFO-daratumumab to determine the sum of cell internalized and surface bound fractions. MM1.S cells were grown in RPMI medium until confluent, harvested and re-suspended in phosphate buffered saline (details in the supplemental file). [89Zr]Zr-DFO-daratumumab (100 μL in phosphate buffered saline) was added to 500 μL of 2.5×10^6 MM1.S cells in Eppendorf tubes and the samples were incubated at 37 °C for 1 h. To determine the non-specific binding, cells were also incubated with 200-fold molar excess of the unmodified unlabeled daratumumab. Following incubation, samples were

centrifuged at 15,000 rpm for 5 min and the radioactive supernatant was removed by vacuum aspiration. Cell pellets were washed twice with 500 µL ice cold phosphate buffered saline and centrifuged for 2 min, supernatant was removed and cell pellets were counted for radioactivity using gamma counter (PerkinElmer Wizard2 Gamma Counter, PerkinElmer, Houston, TX).

Immunoreactivity determination (Lindmo) assay.

The *in vitro* binding characteristics (immunoreactive fraction) of radiolabeled daratumumab was determined by performing the cell binding Lindmo assay as described by Lindmo *et al* (16), with MM1.S myeloma cells. For the antigen binding experiment, MM1.S cells (5x10^6 cells/mL stock solution) were suspended in PBS, and a fixed amount of radioactivity (5,000 cpm) was added to an increasing number of cells (50uL – 500uL). After 1 h of incubation, the cell suspensions were centrifuged and repeatedly washed with PBS containing 1% BSA to determine the radioactive uptake. The specific binding was calculated as the ratio of cell bound radioactivity to the total amount of radioactivity added. All binding experiments were performed in triplicate.

Confocal microscopy

Cells were washed very gently with cold media after treatment and imaged immediately with a Nikon A1Rsi Confocal Microscope [Ex-Em (Hoechst 33342): 405nm-450/40nm; Ex-Em: (GFP) 488nm-530/30 nm; Ex-Em; (Cy5) 640nm-660/20 nm (Ex = laser excitation wavelength; Em = bandpass emission filter wavelength)]. Images were analyzed using ImageJ software (Research Services Branch-National Institute of Health).

Tissue distribution of [89Zr]Zr-DFO-daratumumab in MM1.S tumor-bearing mice

A separate set of mice was used for conducting Mice were sacrificed at 6 or 7 days after administration of the radiolabeled antibody and organs of interest including tumors were harvested, weighed and counted for radioactivity in the gamma counter. Data were background

and decay corrected and percent injected dose per gram (%ID/g) for each tissue sample was calculated.

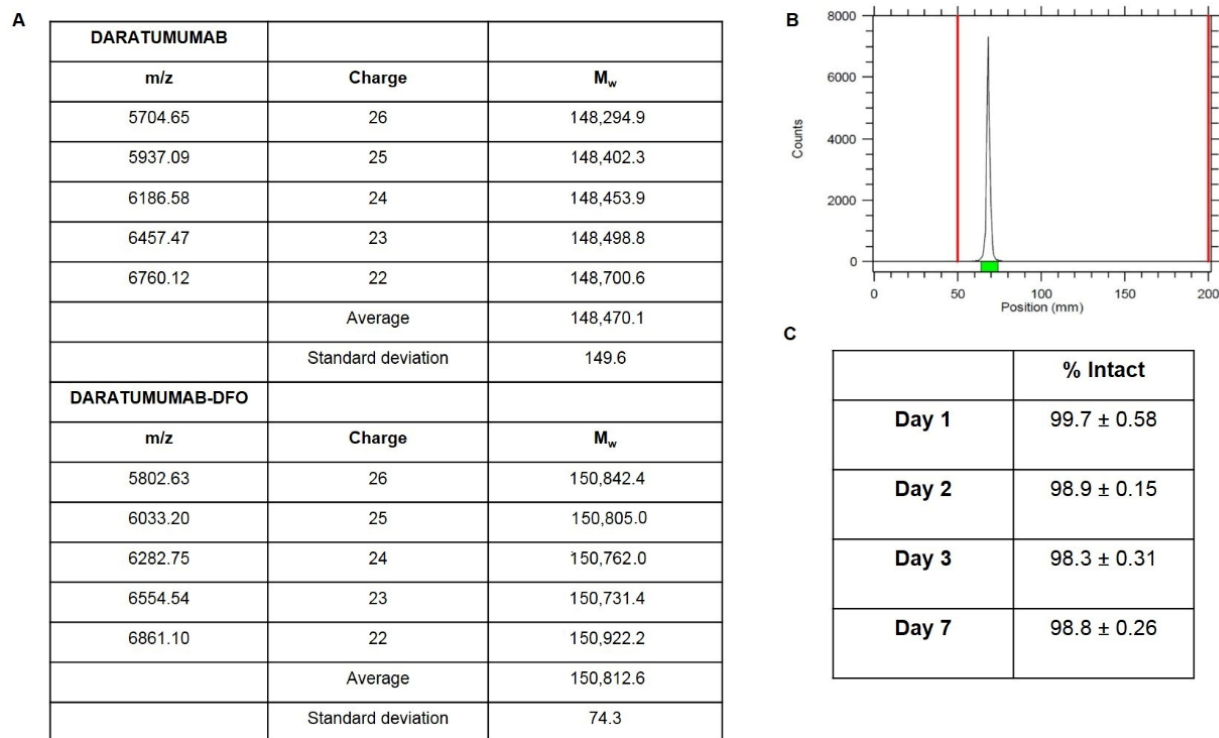**Small animal [89Zr]Zr-DFO-daratumumab-PET/CT imaging**

PET and CT images were acquired at 6 or 7 days after radiotracer injection with the small animal Siemens Inveon PET/CT scanner (Siemens Medical Solutions, Knoxville, TN). Static images were collected for 30 min and co-registered using the Inveon Research Workplace (IRW) software (Siemens Medical Solutions, Knoxville, TN). Regions of interest were selected from PET images using CT anatomical guidelines and the activity associated with the regions of interest was measured with IRW software. Maximum standard uptake values were calculated using standard uptake values = ([MBq/mL] x [animal weight (g)/ [injected dose (MBq)]).

RESULTS

Synthesis and characterization of daratumumab-DFO

The anti-CD38 antibody, daratumumab, was modified with the bifunctional chelator DFO-Bz-NCS with a 15:1 molar excess of chelator to the antibody. The observed molecular weight (M_W) of the unmodified antibody, calculated using ESI mass spectra was 148,470 (±150) Da. The observed M_W was slightly higher than the actual M_W, 145,391 Da. The ~1% error in experimental mass is reasonable as daratumumab is not very stable in gas phase. Based on the ESI-MS of the daratumumab-DFO conjugate, the calculated the m/z was 150,813 (±74) Da. The calculated average number of chelators attached to single antibody molecule was approximately 7 (Supplemental Fig. 1A).
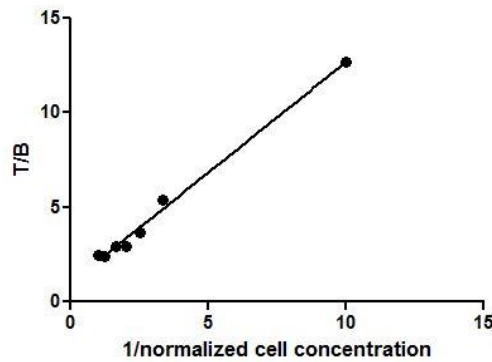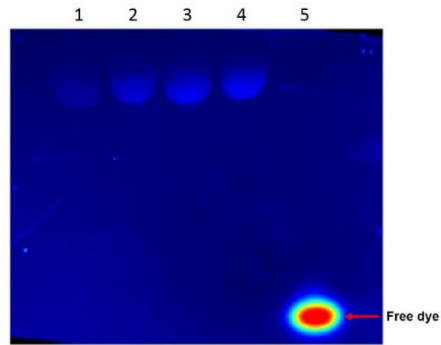
SUPPLEMENTAL FIGURES

A

DARATUMUMAB		
m/z	Charge	M_w
5704.65	26	148,294.9
5937.09	25	148,402.3
6186.58	24	148,453.9
6457.47	23	148,498.8
6760.12	22	148,700.6
	Average	148,470.1
	Standard deviation	149.6
DARATUMUMAB-DFO		
m/z	Charge	M_w
5802.63	26	150,842.4
6033.20	25	150,805.0
6282.75	24	150,762.0
6554.54	23	150,731.4
6861.10	22	150,922.2
	Average	150,812.6
	Standard deviation	74.3

B

C

	% Intact
Day 1	99.7 ± 0.58
Day 2	98.9 ± 0.15
Day 3	98.3 ± 0.31
Day 7	98.8 ± 0.26

Supplemental Figure 1. (A) ESI-MS results for unmodified daratumumab antibody (top) and daratumumab-DFO bio-conjugate (bottom); (B) Radio-TLC of [89Zr]Zr-DFO-daratumumab: mobile phase – 50mM diethylenetriaminepentaacetic acid, (C) *In vitro* serum stability of [89Zr]Zr-DFO-daratumumab at various incubation times.
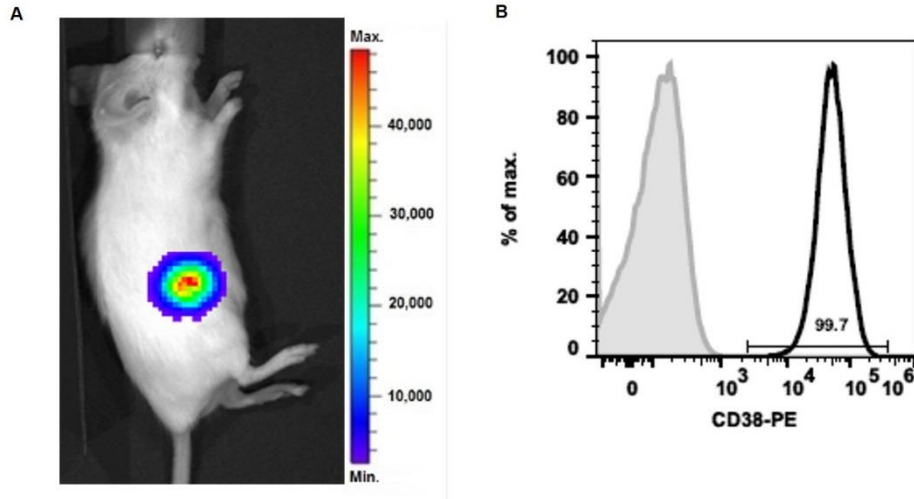
Supplemental Figure 2. (A) Representative BLI image of a SCID mouse bearing s.c MM1.S tumor in the flank. (B) Flow cytometry was performed on the extracted tumor (mouse shown in 2A) that demonstrated high CD38 expression retained on the MM1.S tumors.

Supplemental Figure 3. The immunoreactivity of [89Zr]Zr-DFO-daratumumab was estimated by measuring the binding of a constant concentration of [89Zr]Zr-DFO-daratumumab to increasing numbers of MM1.S multiple myeloma cells that strongly expressed the CD38 antigen. This is a double-inverse plot of a triplicate assay. T/B=Total Activity/Bound Activity

Supplemental Figure 4. Qualitative characterization of daratumumab-Cy5 using SDS-PAGE. Lanes 1-4 represent different equivalents of sulfo-Cy5-NHS ester to daratumumab. Lane 5 is showing the unmodified Sulfo-Cy5-NHS dye.
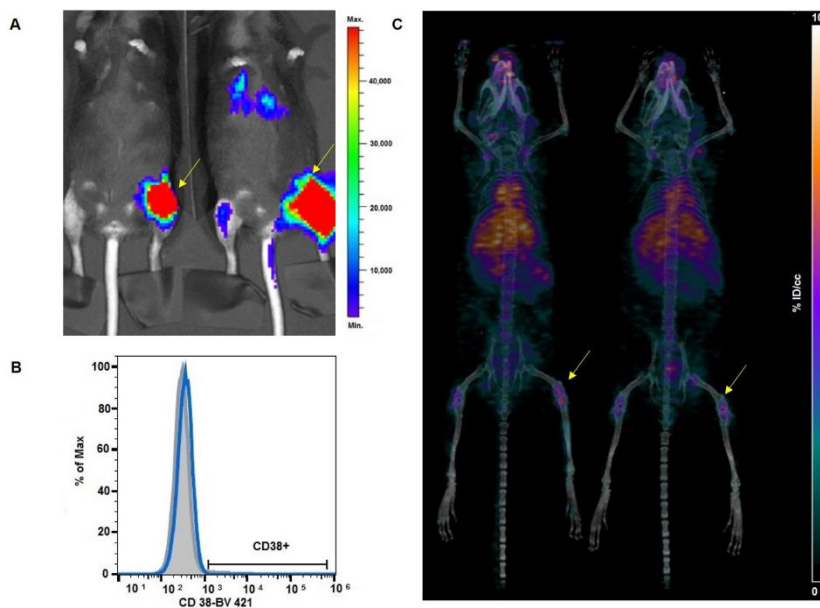
Supplemental Figure 5. (A) Bioluminescence (BLI) images of the intra-tibial 5TGM1-GFP-*luc* (5TGM1) tumor (yellow arrows) bearing KaLwRij mice. (B) Flow cytometry data showed less than 1% CD38-positive expression in murine 5TGM1 MM cells. (C) [89Zr]Zr-DFO-daratumumab/PET/CT MIP images of the i.t. 5TGM1/KaLwRij mice at 7 days post injection of the radiopharmaceutical. [89Zr]Zr-DFO-daratumumab was not-retained by the 5TGM1-KaLwRij tumors *in vivo.*

ORGAN	% ID/g
Blood	11.34 ± 0.25
Lungs	7.14 ± 0.55
Liver	8.68 ± 0.92
Spleen	25.57 ± 3.39
Kidney	6.28 ± 0.64
Muscle	2.17 ± 0.15
Fat	1.45 ± 0.52
Heart	4.13 ± 0.34
Bone	7.93 ± 0.78
Adrenals	4.76 ± 0.54
Pancreas	2.02 ± 0.37
Stomach	0.93 ± 0.23
Sm intestine	1.65 ± 0.18
U large intestine	1.21 ± 0.15
L large intestine	1.13 ± 0.15

Supplemental Table 1: Biodistribution of [89Zr]Zr-DFO-daratumumab in non-tumor control wild-type SCID mice (n=4) at 7 days post administration of the radiotracer.

Organs	[89Zr]Zr-DFO-daratumumab (%ID/g)	[89Zr]Zr-DFO-daratumumab+Block (%ID/g)
Blood	11.05 ± 1.38	12.19 ± 1.49
Lungs	8.58 ± 1.73	8.84 ± 0.10
Liver	9.16 ± 1.47	7.53 ± 2.16
Spleen	31.51 ± 6.10	10.57 ± 1.44
Kidney	7.06 ± 1.11	7.28 ± 2.23
Muscle	2.25 ± 0.32	2.54 ± 0.81
Fat	2.21 ± 0.99	1.71 ± 0.82
Heart	4.15 ± 0.35	4.23 ± 0.91
Bone	8.94 ± 0.68	5.54 ± 1.07
Adrenals	5.46 ± 2.96	4.73 ± 2.16
Pancreas	2.20 ± 0.30	2.16 ± 0.44
Stomach	1.53 ± 0.46	1.51 ± 0.44
Sm intestine	1.91 ± 0.28	1.85 ± 0.35
U large intestine	1.94 ± 0.55	1.89 ± 0.30
L large intestine	1.39 ± 0.44	1.74 ± 0.61
Tumor	27.7 ± 7.6	6.46 ± ND

Supplemental Table 2: Biodistribution of [89Zr]Zr-DFO-dararumumab in CD38$^+$ MM1.S xenografts (n=3) at 7 d post administration of the radiotracer. A set of animals was co-injected with 200-fold excess of unlabeled daratumumab.